

Velocity Distribution in a Viscous Granular Gas

Alexandre Rosas^{1,2}, Daniel ben-Avraham³, and Katja Lindenberg^{1,4}

¹*Department of Chemistry and Biochemistry, University of California San Diego, La Jolla, CA 92093-0340*

²*Departamento de Física, Universidade Federal da Paraíba, João Pessoa, PB 58.059-970, Brazil*

³*Physics Department, Clarkson University, Potsdam NY 13699-5820*

⁴*Institute for Nonlinear Science, University of California San Diego, La Jolla, CA 92093-0340*

We investigate the velocity relaxation of a viscous one-dimensional granular gas, that is, one in which neither energy nor momentum is conserved in a collision. Of interest is the distribution of velocities in the gas as it cools, and the time dependence of the relaxation behavior. A Boltzmann equation of instantaneous binary collisions leads to a two-peaked distribution with each peak relaxing to zero velocity as $1/t$ while each peak also narrows as $1/t$. Numerical simulations of grains on a line also lead to a double-peaked distribution that narrows as $1/t$. A Maxwell approximation leads to a single-peaked distribution about zero velocity with power-law wings. This distribution narrows exponentially. In either case, the relaxing distribution is not of Maxwell-Boltzmann form.

PACS numbers: 45.70.-n, 05.20.Dd, 05.70.Ln, 83.10.Rs

I. INTRODUCTION

Velocity distributions in dilute granular gases are generically away from equilibrium because the collision processes in such gases are dissipative. Even in the dilute limit the velocities of different particles may be strongly correlated [1], and therefore the usual description in terms of single particle distribution functions may not be sufficient to determine all the properties of the granular gas. Nevertheless, the single particle distribution $P(r, v, t)$ contains important information, and is particularly interesting because in a granular gas it typically deviates from the Maxwell-Boltzmann distribution. Quite aside from possible spatial inhomogeneity effects such as particle clustering, even the single particle velocity distribution $P(v, t)$ in general differs from the Maxwell-Boltzmann form. The deviations of these single particle distributions from the usual “universal” behavior in ordinary gases has been a subject of intense interest in recent years [2, 3, 4, 5, 6]. These deviations can be observed in granular gases that achieve a steady state because external forcing balances the dissipative collisions among particles [7], or they can be observed in unforced gases as they cool down [8, 9, 10, 11].

Typically, gases equilibrate or achieve a steady state via collision processes. Conservation of energy and momentum imply Maxwellian velocity statistics in three dimensions [12]. In lower dimensions the situation is more complicated; for example, a gas of hard spheres in one dimension simply retains its initial distribution forever. In granular media the situation is in any case more complex because energy is certainly not conserved [13]. Most work on relaxation in granular materials, in any dimension, has focused on the interesting consequences of energy non-conservation. In the presence of friction, not only is energy not conserved, but momentum is not conserved either, leading to interesting new relaxation behavior [7, 14, 15, 16]. In fact, we have recently shown [16] that in the absence of conservation laws random linear mixing can lead to velocity distributions with algebraic

or exponential tails, with nontrivial characteristic exponents. In general, conservation laws play a crucial role in the universality of the usual velocity distribution properties.

Our focus here is the effect of viscosity, and consequently, of momentum non-conservation, on the velocity distribution as a one-dimensional dilute granular gas cools down. The model consists of N grains on a line (or a circle, since we will use periodic boundary conditions). The grains move freely except during collisions, governed by the Hertz potential,

$$\begin{aligned} V(\delta_{k,k+1}) &= \frac{a}{n} |\delta_{k,k+1}^n|, & \delta \leq 0, \\ V(\delta_{k,k+1}) &= 0, & \delta > 0. \end{aligned} \quad (1)$$

Here $\delta_{k,k+1} \equiv y_{k+1} - y_k$, y_k is the displacement of granule k from its equilibrium position, and a is a prefactor determined by Young’s modulus and Poisson’s ratio. The exponent n is $5/2$ for spheres, it is 2 for cylinders, and in general depends on geometry. In this paper we only consider cylindrical grains, which leads to considerable simplification while still capturing important general features of the non-Maxwellian distributions. We stress that the one-sided (only repulsion) granular potential even with $n = 2$ is entirely different from a two-sided (repulsion and attraction) harmonic potential.

The displacement of the k -th granule ($k = 1, 2, \dots, N$) of mass m in the chain from its equilibrium position in a frictional medium is governed by the equation of motion

$$\begin{aligned} m \frac{d^2 y_k}{d\tau^2} &= -\tilde{\gamma} \frac{dy_k}{d\tau} \\ &- a(y_k - y_{k+1})^{n-1} \theta(y_k - y_{k+1}) \\ &+ a(y_{k-1} - y_k)^{n-1} \theta(y_{k-1} - y_k). \end{aligned} \quad (2)$$

Here $\tilde{\gamma}$ is the friction coefficient and $\theta(y)$ is the Heaviside function, $\theta(y) = 1$ for $y > 0$, $\theta(y) = 0$ for $y < 0$, and $\theta(0) = 1/2$. The Heaviside function ensures that two particles interact only when in contact, that is, only when

the particles are loaded. Note that for periodic boundary conditions $y_{k+N} = y_k$. In terms of the rescaled variables and parameters

$$y_k = C_n x_k, \quad \tau = \frac{1}{v_0} C_n t, \quad \gamma = \frac{\tilde{\gamma}}{mv_0} C_n, \quad (3)$$

where $C_n \equiv (mv_0^2/a)^{1/n}$, Eq. (2) can be rewritten as

$$\begin{aligned} \ddot{x}_k = & -\gamma \dot{x}_k - (x_k - x_{k+1})^{n-1} \theta(x_k - x_{k+1}) \\ & + (x_{k-1} - x_k)^{n-1} \theta(x_{k-1} - x_k). \end{aligned} \quad (4)$$

A dot denotes a derivative with respect to t . The velocity v_0 is an arbitrary choice in terms of which other velocities are now expressed, i.e., it settles the energy scale of the system.

Although the problem might appear relatively simple because it is one-dimensional and quasi-linear, the one-sidedness of the potential leads to analytic complexities even in the dissipationless case [15, 17, 18], and even greater complexities in the presence of dissipation [14, 15]. Our purpose in this paper is to explore analytic approximations appropriate for *low densities*. The low density feature of these approximations is implemented via the assumption that the collisions are always *binary*, that is, that only two granules at a time are members of any collision event, and that at any moment of time there is at most one collision.

We explore two low-density analytic approximations. One is based on the Boltzmann equation for binary collisions, presented in Sec. II and elaborated in Sec. III, and the other is an even simpler model that we call the Maxwell model, presented in Sec. IV. The detailed description of a binary collision that must be used as an input in either of these models is also presented in Sec. II. To assess the success of each analytic model, a comparison of the approximate model results with numerical simulations of the entire chain is carried out in Sec. V. In that section we also summarize the outcome of our analysis.

II. BOLTZMANN EQUATION AND COLLISIONS

Our analytic starting point in the following sections is the Boltzmann equation for binary collisions in a spatially uniform gas, which describes the rate of change of the probability distribution of velocities, $P(v, t)$. If u_1 and u_2 are the initial velocities of a pair of particles just before a collision and u'_1 and u'_2 their velocities just after, then the Boltzmann equation is

$$\begin{aligned} \frac{\partial}{\partial t} P(v, t) = & \iint du_1 du_2 |u_1 - u_2| P(u_1, t) P(u_2, t) \\ & \times [\delta(v - u'_1) + \delta(v - u'_2) - \delta(v - u_1) - \delta(v - u_2)]. \end{aligned} \quad (5)$$

Since the problem is one-dimensional, one can keep track of the precise conditions under which a collision between

two particles of given velocities will or will not occur, and how these events will change the distribution function.

The binary collision approximation implies that at any one time there is at most one pair of loaded grains, so we need to consider in detail the fate of a colliding pair from the beginning to the end of a collision [14]. At the moment of the start of the collision, which we call $t = 0$, the velocities of the grains are u_1 and u_2 . The collision ends at the time $\tau = 2\pi/\sqrt{8 - \gamma^2}$, when the grains lose contact. It is important to notice that for $n = 2$ the collision time is *independent* of the initial condition. This is a feature that makes the cylindrical granule geometry much simpler than other shapes. Without loss of generality we take $u_1 > u_2$, since we can always relabel particles to make it so. The velocities at the moment of separation τ are found to be [14]

$$\begin{aligned} u'_1 = & u_1 \frac{\mu^2 - \mu}{2} + u_2 \frac{\mu^2 + \mu}{2}, \\ u'_2 = & u_1 \frac{\mu^2 + \mu}{2} + u_2 \frac{\mu^2 - \mu}{2}, \end{aligned} \quad (6)$$

where $\mu \equiv e^{-\gamma\tau/2}$.

In our further analysis we think of the distance traveled by the granules during a collision as negligible. For small damping γ this distance is $(u_1 + u_2)\pi/\sqrt{8}$, which is to be compared to the mean distance between particles. The latter can be made arbitrarily large by lowering the density. We also take the collision time between two granules as instantaneous. This collision time for small damping is $\tau \approx \pi/\sqrt{2}$, to be compared with the typical mean free time of flight of a particle between collisions. With these approximations, the only role played by the viscosity is dictated by the collision rule (6). These assumptions might conceivably be problematic for the most energetic particles that may travel a relatively long distance during a collision and a relatively short distance between collisions, but explicit analysis of these extreme events is difficult and probably not important at sufficiently low densities.

III. BOLTZMANN PROBLEM

We now start with the Boltzmann equation (5) in which the collision rate depends on the difference in the velocities of the colliding pair. To write the explicit Boltzmann equation for our system, we must collect all the instances that lead to a collision, that is, all the instances for which one or another of the δ -functions in Eq. (5) can be satisfied. There are six possible events that contribute to a change in $P(v, t)$. We list the contribution to $\partial P/\partial t$ from each event:

$$(a) (v, u) \rightarrow (u'_1, u'_2); \quad v > u$$

Implementing the third δ -function in Eq. (5) we find

$$\left[\frac{\partial}{\partial t} P(v, t) \right]_{(a)} = -P(v, t) \int_{-\infty}^v du (v - u) P(u, t). \quad (7)$$

(b) $(u, v) \rightarrow (u'_1, u'_2); \quad u > v$

Implementation of the fourth δ -function in Eq. (5) leads to

$$\left[\frac{\partial}{\partial t} P(v, t) \right]_{(b)} = -P(v, t) \int_v^\infty du (u - v) P(u, t). \quad (8)$$

(c) $(u_1, u_2) \rightarrow (v, u'_2); \quad u_1 > u_2$

Here we implement the first δ -function in Eq. (5) to find

$$\begin{aligned} \left[\frac{\partial}{\partial t} P(v, t) \right]_{(c)} &= \int_{-\infty}^{v/\mu^2} \left(\frac{2v}{\mu^2 - \mu} - \frac{2\mu^2 u}{\mu^2 - \mu} \right) \\ &\times P \left(\frac{2v}{\mu^2 - \mu} - \frac{(\mu^2 + \mu)u}{\mu^2 - \mu}, t \right) P(u, t) du. \end{aligned} \quad (9)$$

(d) $(u_1, u_2) \rightarrow (v, u'_2); \quad u_1 < u_2$

We again implement the first δ -function in Eq. (5):

$$\begin{aligned} \left[\frac{\partial}{\partial t} P(v, t) \right]_{(d)} &= \int_{v/\mu^2}^\infty \left(\frac{2\mu^2 u}{\mu^2 - \mu} - \frac{2v}{\mu^2 - \mu} \right) \\ &\times P \left(\frac{2v}{\mu^2 - \mu} - \frac{(\mu^2 + \mu)u}{\mu^2 - \mu}, t \right) P(u, t) du. \end{aligned} \quad (10)$$

(e) $(u_1, u_2) \rightarrow (u'_1, v); \quad u_1 > u_2$

Now we implement the second δ -function in Eq. (5):

$$\begin{aligned} \left[\frac{\partial}{\partial t} P(v, t) \right]_{(e)} &= \int_{v/\mu^2}^\infty \left(\frac{2\mu^2 u}{\mu^2 + \mu} - \frac{2v}{\mu^2 + \mu} \right) \\ &\times P \left(\frac{2v}{\mu^2 + \mu} - \frac{(\mu^2 - \mu)u}{\mu^2 + \mu}, t \right) P(u, t) du. \end{aligned} \quad (11)$$

(f) $(u_1, u_2) \rightarrow (u'_1, v); \quad u_1 < u_2$

Again we implement the second δ -function in Eq. (5):

$$\begin{aligned} \left[\frac{\partial}{\partial t} P(v, t) \right]_{(f)} &= \int_{-\infty}^{v/\mu^2} \left(\frac{2v}{\mu^2 + \mu} - \frac{2\mu^2 u}{\mu^2 + \mu} \right) \\ &\times P \left(\frac{2v}{\mu^2 + \mu} - \frac{(\mu^2 - \mu)u}{\mu^2 + \mu}, t \right) P(u, t) du. \end{aligned} \quad (12)$$

The full equation for $\partial P(v, t)/\partial t$ is the sum of these six contributions. While the collisions of types (a) and (b) decrease the probability density $P(v, t)$, collisions (c) to (f) increase it.

We assume a scaling solution of the form,

$$P(v, t) = \frac{1}{\phi(t)} F \left(\frac{v}{\phi(t)} \right), \quad (13)$$

and define

$$x \equiv \frac{v}{\phi(t)}, \quad y \equiv \frac{u}{\phi(t)}. \quad (14)$$

The Boltzmann equation then is

$$\begin{aligned} \frac{\partial P(v, t)}{\partial t} &= -\frac{\dot{\phi}(t)}{\phi^2(t)} (F(x) + xF'(x)) \\ &= -\int_{-\infty}^x (x - y) F(x) F(y) dy \\ &\quad - \int_x^\infty (y - x) F(x) F(y) dy \\ &\quad + \int_{-\infty}^{x/\mu^2} \left(\frac{2x}{\mu^2 - \mu} - \frac{2\mu^2 y}{\mu^2 - \mu} \right) \\ &\quad \times F \left(\frac{2x}{\mu^2 - \mu} - \frac{(\mu^2 + \mu)y}{\mu^2 - \mu} \right) F(y) dy \\ &\quad + \int_{x/\mu^2}^\infty \left(\frac{2\mu^2 y}{\mu^2 - \mu} - \frac{2x}{\mu^2 - \mu} \right) \\ &\quad \times F \left(\frac{2x}{\mu^2 - \mu} - \frac{(\mu^2 + \mu)y}{\mu^2 - \mu} \right) F(y) dy \\ &\quad + \int_{x/\mu^2}^\infty \left(\frac{2\mu^2 y}{\mu^2 + \mu} - \frac{2x}{\mu^2 + \mu} \right) \\ &\quad \times F \left(\frac{2x}{\mu^2 + \mu} - \frac{(\mu^2 - \mu)y}{\mu^2 + \mu} \right) F(y) dy \\ &\quad + \int_{-\infty}^{x/\mu^2} \left(\frac{2x}{\mu^2 + \mu} - \frac{2\mu^2 y}{\mu^2 + \mu} \right) \\ &\quad \times F \left(\frac{2x}{\mu^2 + \mu} - \frac{(\mu^2 - \mu)y}{\mu^2 + \mu} \right) F(y) dy. \end{aligned} \quad (15)$$

Defining $z = \frac{2x}{\mu^2 - \mu} - \frac{(\mu^2 + \mu)y}{\mu^2 - \mu}$ and recognizing that the dummy variable z can be relabeled as y after the transformation, one finds that the third term on the right hand side of this equation becomes proportional to the fourth, and the fifth to the sixth, so that these pairs can be combined to yield the simpler expression

$$\begin{aligned} -\frac{\dot{\phi}(t)}{\phi^2(t)} (F(x) + xF'(x)) &= -\int_{-\infty}^x (x - y) F(x) F(y) dy \\ &\quad - \int_x^\infty (y - x) F(x) F(y) dy \\ &\quad + \frac{2}{\mu + 1} \int_{-\infty}^{x/\mu^2} \left(\frac{2x}{\mu^2 + \mu} - \frac{2\mu^2 y}{\mu^2 + \mu} \right) \\ &\quad \times F \left(\frac{2x}{\mu^2 + \mu} - \frac{(\mu^2 - \mu)y}{\mu^2 + \mu} \right) F(y) dy \\ &\quad + \frac{2}{\mu + 1} \int_{x/\mu^2}^\infty \left(\frac{2\mu^2 y}{\mu^2 + \mu} - \frac{2x}{\mu^2 + \mu} \right) \\ &\quad \times F \left(\frac{2x}{\mu^2 + \mu} - \frac{(\mu^2 - \mu)y}{\mu^2 + \mu} \right) F(y) dy. \end{aligned} \quad (16)$$

Since the only explicit time dependence resides in the $\frac{\dot{\phi}(t)}{\phi^2(t)}$ term, this term must be constant. Integrating this

term leads to $\phi(t) = \frac{\phi(0)}{1+ct}$, where c is a constant. Therefore, asymptotically,

$$\phi(t) \sim t^{-1}. \quad (17)$$

We have not found an analytic solution to Eq. (16). We therefore simulate the equation numerically (next subsection) and implement a further approximation that leads to an analytic solution that we can compare with the numerical results (subsequent subsection).

A. Simulation of the Boltzmann equation

We directly simulate the Boltzmann equation using the following algorithm:

1. We start with N grains whose velocities are independently assigned accordingly to an initial distribution $P(v, 0)$.
2. We choose one pair of grains with probability proportional to the modulus of their relative velocity and let them collide, using the collision rule 6.
3. Time is incremented by twice the inverse of the modulus of the pre-collisional relative velocity. The factor of 2 accounts for picked pairs that do not collide, since our algorithm forces a collision at each step.
4. We iterate steps 1 to 3 many times and for many samples.

In our simulations we took $N = 100$ and averaged our results over 1000 samples. In Fig. 1 we show the resulting velocity distribution for $\gamma = 0.9$ at different times. It is clear that the initial symmetric and single peaked distribution develops two distinct peaks as it starts to collapse to the ultimate equilibrium distribution, a δ -function at $v = 0$. Moreover, in Fig. 2 we show that the width of the distribution and the width of each peak both decay as $1/t$. In the simulation underlying this figure the initial distribution was a double peaked Gaussian, chosen because it converges quickly. We find the same asymptotic behavior for the initially exponential distribution, namely, that each peak moves inward as $1/t$ and also shrinks as $1/t$. The validity of the scaling solution Eq. (13) is clearly evident in the scaled rendition of the velocity distribution shown in Fig. 3 for different times.

B. Two-particle model

While the Boltzmann equation (16) does not appear amenable to analytic solution, we can formulate a simpler model that may incorporate the main effects of the system. In this model we have an ensemble of rings of size l each containing only two particles. In each ring, the dynamics is perfectly deterministic: the two balls will

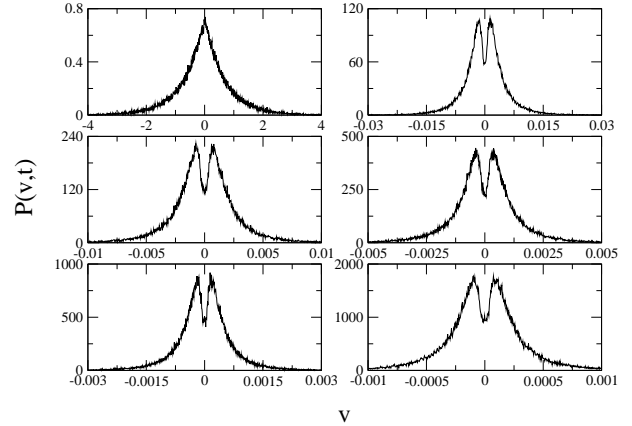


FIG. 1: Velocity distribution obtained using the simulation algorithm detailed in Sec. III A. From left to right and top to bottom, the panels correspond to time 0, 8000, 16000, 32000, 64000 and 128000 in the adimensional units used in this paper. The initial distribution is a symmetric exponential. Notice the change in the scales as time proceeds.

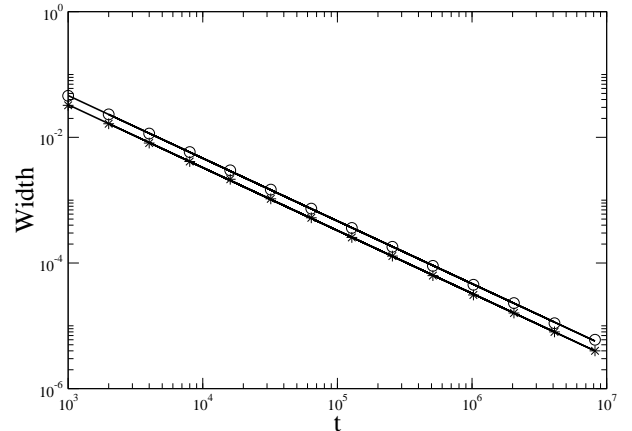


FIG. 2: Width of the velocity distribution (circles) and the width of each peak (stars). The lines represent the best fit of the width vs time for the full distribution (exponent -0.998) and for each peak (exponent -1.001).

keep colliding with each other, back and forth, moving toward each other with ever decreasing velocities. For each one ring, after n collisions, the velocities, which we call u_n and v_n , are obtained by repeated application of the collision rule (6),

$$\begin{aligned} u_n &= \frac{\mu^{2n} + (-\mu)^n}{2} u_0 + \frac{\mu^{2n} - (-\mu)^n}{2} v_0, \\ v_n &= \frac{\mu^{2n} - (-\mu)^n}{2} u_0 + \frac{\mu^{2n} + (-\mu)^n}{2} v_0, \end{aligned} \quad (18)$$

where u_0 and v_0 are the initial velocities. Note that each of these velocities alternates from positive to negative as the particles move in one direction and then another

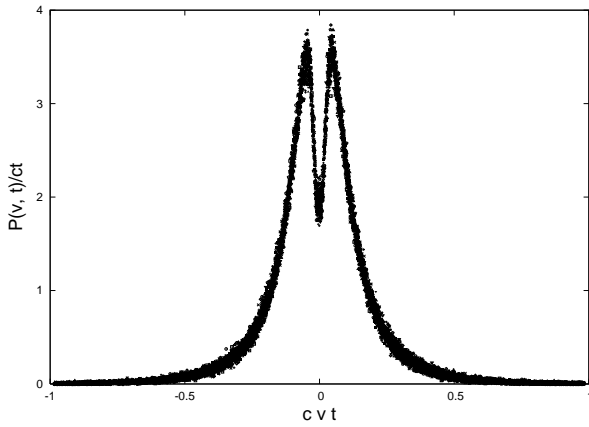


FIG. 3: Asymptotic behavior of the scaled velocity distribution. Different symbols stand for different times (1000×2^n with $n = 0, 1, \dots, 13$). The constant c in the figure is arbitrary and was chosen to facilitate comparison with Fig. 8.

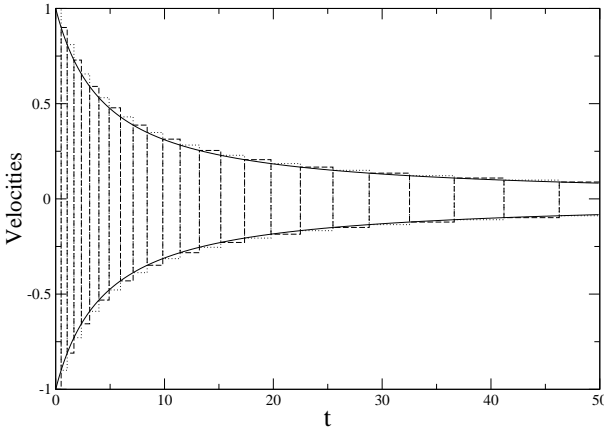


FIG. 4: Dashed lines and dotted lines are respectively velocities u_n and v_n on a ring with two particles, with $u_0 = -v_0 = 1$ and $l = 1$. The solid curves are the envelopes $A(t)$ (upper) and $B(t)$ (lower).

in the ring, as illustrated in Fig. 4. The time that has elapsed by the n^{th} collision is obtained as follows. Since the grains are in a ring, the distance they have to travel between two collisions is l . The travel time is $l/|u - v|$, where u and v are their current velocities between collisions. Hence,

$$t_n = \frac{l}{|u_0 - v_0|} \sum_{k=0}^{n-1} \mu^{-k} = \frac{l}{|u_0 - v_0|} \frac{\frac{1}{\mu^n} - 1}{\frac{1}{\mu} - 1} \quad (19)$$

The sign alternation of the velocities in Eq. (18) is not important in the effort to understand the long time behavior of the distribution. We can approximate the velocities by envelope functions $A(t)$ (upper curve) and

$B(t)$ (lower curve), as illustrated in Fig. 4:

$$\begin{aligned} u_n &= A(t)u_0 + B(t)v_0, \\ v_n &= B(t)u_0 + A(t)v_0. \end{aligned} \quad (20)$$

The initial velocities u_0 and v_0 are arbitrary, and have only been chosen of equal magnitude for purposes of illustration in the figure. The envelope functions can be found by solving Eq. (19) for μ^n , substituting this into Eq. (18) ignoring the minus signs in the $(-\mu)^n$ factors, and setting $t_n \equiv t$. One finds

$$\begin{aligned} A(t) &= \frac{1}{2} \left[1 + \frac{|u_0 - v_0|}{l} \left(\frac{1}{\mu} - 1 \right) t \right]^{-2} \\ &\quad + \frac{1}{2} \left[1 + \frac{|u_0 - v_0|}{l} \left(\frac{1}{\mu} - 1 \right) t \right]^{-1}, \end{aligned} \quad (21)$$

$$\begin{aligned} B(t) &= \frac{1}{2} \left[1 + \frac{|u_0 - v_0|}{l} \left(\frac{1}{\mu} - 1 \right) t \right]^{-2} \\ &\quad - \frac{1}{2} \left[1 + \frac{|u_0 - v_0|}{l} \left(\frac{1}{\mu} - 1 \right) t \right]^{-1}. \end{aligned}$$

Hence, if initially the particles had a velocity distribution $P(v, 0)$, then the velocity distribution as a function of time is

$$\begin{aligned} P(v, t) &= \iint \delta(v - A(t)u_0 - B(t)v_0) \\ &\quad \times P(u_0, 0)P(v_0, 0)du_0dv_0. \end{aligned} \quad (22)$$

Asymptotically,

$$A(t) = -B(t) \sim \frac{1}{2} \frac{l}{|u_0 - v_0|t} \left(\frac{1}{\mu} - 1 \right)^{-1}, \quad (23)$$

so that

$$\begin{aligned} P(v, t) &= \iint \delta \left(v - \frac{1}{2} \frac{l}{t} \left(\frac{1}{\mu} - 1 \right)^{-1} \operatorname{sgn}(u_0 - v_0) \right) \\ &\quad \times P(u_0, 0)P(v_0, 0)du_0dv_0. \end{aligned} \quad (24)$$

Therefore, $P(u, t)$ consists of two δ -peaks, one at positive and one at negative velocities. If the initial distribution is symmetric about zero velocity and is properly normalized, then

$$\begin{aligned} P(v, t) &\sim \frac{1}{2} \delta \left(v - \frac{l}{2t} \left(\frac{1}{\mu} - 1 \right)^{-1} \right) \\ &\quad + \frac{1}{2} \delta \left(v + \frac{l}{2t} \left(\frac{1}{\mu} - 1 \right)^{-1} \right). \end{aligned} \quad (25)$$

The peaks thus move toward the final velocity $u = 0$ as $1/t$. This time dependence is in agreement with the Boltzmann equation analysis.

The two δ -peaks here reflect the fact that the magnitude of the velocity difference between the colliding particles eventually becomes independent of the magnitude of the initial velocity difference. Clearly, in the Boltzmann equation analysis this is not quite the case and the peaks have a finite width as they converge. However, this width decreases in time as $1/t$, approaching the behavior of the two-particle ring model asymptotically.

IV. MAXWELL PROBLEM

In the Boltzmann equation, the rate of collision of a pair of particles depends on their relative velocity. The “Maxwell problem” further assumes that the pair of colliding grains is chosen randomly, all pairs colliding with the same probability at unit rate. The evolution equation (5) for the distribution of velocities is then replaced by the even simpler form

$$\begin{aligned} \frac{\partial}{\partial t} P(v, t) &= \int \int du_1 du_2 P(u_1, t) P(u_2, t) \\ &\times [\delta(v - u'_1) + \delta(v - u'_2) \\ &- \delta(v - u_1) - \delta(v - u_2)]. \end{aligned} \quad (26)$$

This problem with a completely general linear collision rule (of which Eq. (6) is a special case) was analyzed in [16]. In the language used here, if we assume a scaling form as in Eq. (13), we arrive at an equation parallel to Eq. (5) but now with the time-dependent factor $-\dot{\phi}(t)/\phi(t)$. Again, we argue that this term must be a constant, and integration leads to an exponential decay of the width of the distribution instead of the power law found in the Boltzmann case,

$$\phi(t) \sim e^{-\alpha t}. \quad (27)$$

The decay constant depends on the friction coefficient γ . In [16] we described in detail how to evaluate α , and in Fig. 5 we show the resulting values of α . Furthermore, in [16] we also analyzed the shape of the distribution. We found that (regardless of the initial distribution provided that the initial average velocity is zero) $F(x)$ has a single peak around $x = 0$ instead of the double-peaked structure that we find for the Boltzmann problem and its two-ring simplification, and that it has algebraic tails that decay as $F(x) \sim x^{-\nu-1}$. The exponent ν is also a function of γ , as shown in Fig. 5.

V. NUMERICAL SIMULATIONS AND CONCLUSIONS

The two approximations presented in the previous sections lead to very different results for the velocity relaxation behavior of a damped one-dimensional granular

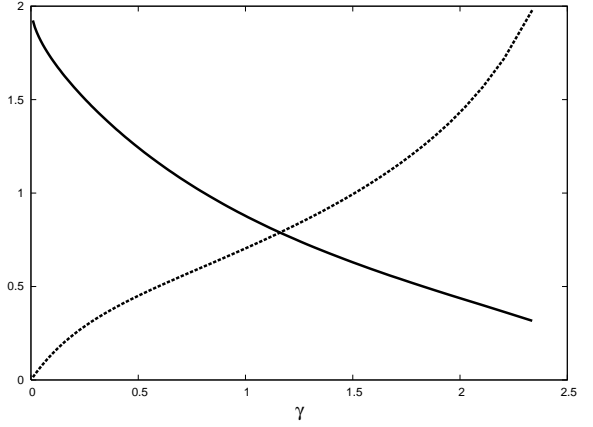


FIG. 5: Exponential decay parameter α (dashed curve), and algebraic decay parameter ν for the tails of the distribution (solid curve), both as a function of viscosity γ .

system. One (Boltzmann problem) leads to a velocity distribution that is double-peaked, with one at positive and one at negative velocities, the peaks moving inward as $1/t$ toward a zero final velocity. The width of the peaks also decreases as $1/t$. The second model (Maxwell problem) leads to a distribution that is single-peaked, with a width that decreases exponentially in time and distribution tails that decay algebraically. Neither of these approximations considers the possible effects of the spatial distribution of granules.

In order to assess the validity of these approximations, and also to get a sense of the possible effects of the spatial distribution of granules, we have carried out numerical simulations of a full chain of particles. Our collision rules are still as indicated in Eq. (6), and, as before, we assume collisions to be instantaneous, but now we actually place the granules on a line and keep track of their positions so that spatial inhomogeneities can occur if the system is so inclined. Results for 10000 granules averaged over 100 simulations are shown in Fig. 6. The particle density is 10^{-3} with the particles initially distributed uniformly. The initial distribution is taken to be a symmetric exponential, and $\gamma = 0.9$. As time proceeds, the initial single peak splits into two peaks which move inward and become narrower, as predicted in our Boltzmann analysis. Both the inward motion of the peaks and the width of the peaks change as $1/t$, as in the Boltzmann approximation (see Fig. 7).

We also tested the scaling hypothesis Eq. 13 on our simulations. In Fig. 8 we show that, as in the Boltzmann approximation, the scaling works quite well. Moreover, in this case, the data can be fitted by a double Γ -distribution

$$F(x) = \frac{1}{2b_1 \Gamma(b_2)} \left| \frac{x}{b_1} \right|^{b_2-1} e^{-\left| \frac{x}{b_1} \right|}. \quad (28)$$

Note that this distribution has only two (γ -dependent) free parameters, b_1 , which sets the scale, and b_2 , which

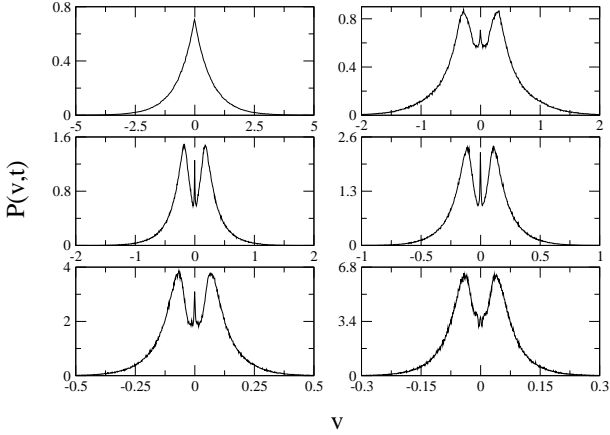


FIG. 6: Velocity distribution obtained from numerical simulations on a line with 10000 granules averaged over 100 realizations. The particle density is 0.001, the initial spatial distribution is uniform, and the initial velocity distribution is a symmetric exponential. The damping parameter $\gamma = 0.9$. From left to right and top to bottom, time is 1000, 8000, 16000, 32000, 64000 and 128000 in adimensional units. Notice the change in the scales as time proceeds.

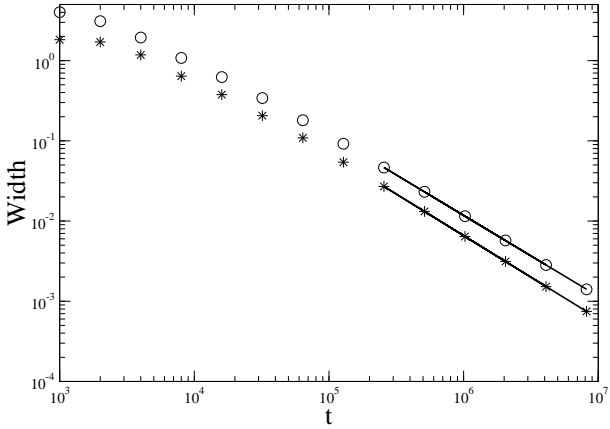


FIG. 7: Width of the velocity distribution (circles) and the width of each peak (stars). The lines represent the best fit of the width vs time for the full distribution (exponent -1.009) and for each peak (exponent -1.035). The initial velocity distribution was a double Gaussian.

sets the shape. In Fig. 8 we plot this distribution for $\gamma = 0.9$ ($b_1 = 0.046$ and $b_2 = 2.637$) together with the simulation data obtained with a double Gaussian initial velocity distribution. We have tested the double Γ -distribution fit for other values of γ , with equal success.

Comparing the velocity distribution for the Boltzmann approximation (Figs. 1 and 3) and the simulations in a line (Figs. 6 and 8) we note that the Boltzmann model converges to the scaling distribution much more rapidly. Initially the simulation results exhibit the same behavior as the Boltzmann model, but for longer times the behav-

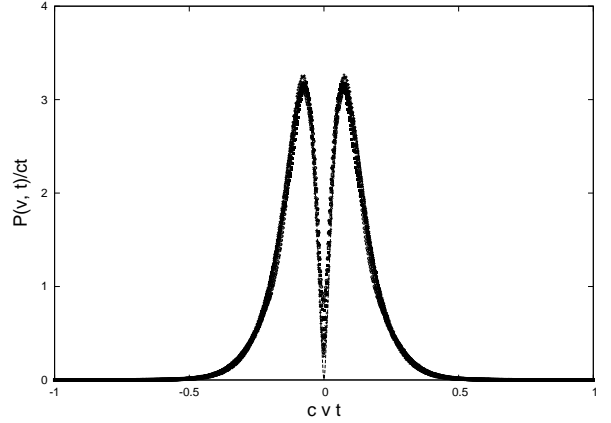


FIG. 8: Asymptotic behavior of the scaled velocity distribution. Different symbols stand for different times (1000×2^n with $n = 7, 8, \dots, 13$) and the dashed line is the best fit of a double gamma distribution. The constant c in the figure is arbitrary and was chosen to facilitate comparison with Fig. 3.

ior of the two distributions for small velocities begin to differ. In the Boltzmann case, the probability of finding a slow granule is much greater than in the simulation.

We conclude from these results that

1. The Maxwell problem is an inadequate representation of the velocity relaxation properties of the granular chain described in Eq. (4). The predicted shape of the distribution does not agree with that of the physical chain.
2. The Boltzmann problem in which we have disregarded spatial dependences captures many of the essential features of the velocity relaxation, the most important and new feature being the appearance of two peaks in the velocity distribution. The Boltzmann problem and even the simpler two-particle simplification of the problem also capture the time dependence of convergence of the two peaks into a single one at zero velocity. The slow ($1/t$) convergence is due to the fact that the collision rate in the Boltzmann picture slows down as the gas cools. By way of contrast, the collision rate in the Maxwell problem does not, leading to an exponential relaxation in time.
3. The Boltzmann approximation does not correctly capture the late time distribution of the slowest particles. This is probably due to spatial correlations that have been ignored in this approximation and that are currently under investigation [19].

We point out again that even in our most complete simulations we have approximated the collision events as instantaneous. While we do not believe this to be a perceptible source of error, it would be interesting (but extremely time consuming) to carry our full simulations of the model Eq. (4) with no further approximations.

Acknowledgments

This work was supported by the Engineering Research Program of the Office of Basic Energy Sciences at the U.

S. Department of Energy under Grant No. DE-FG03-86ER13606 (KL) and by NSF Grant No. PHY-0140094 (DbA).

-
- [1] S. J. Moon, M. D. Shattuck, and J. B. Swift, Phys. Rev. E **64**, 031303 (2001).
- [2] S. Warr, J. M. Huntley, and George T. H. Jacques, Phys. Rev. E **52**, 5583 (1995).
- [3] J. S. Olafsen and J. S. Urbach, Phys. Rev. Lett. **81**, 4369 (1998).
- [4] W. Losert, D. G. W. Cooper, J. Delour, A. Kudrolli, and J. P. Gollub, Chaos **9**, 682 (1999).
- [5] A. Kudrolli and J. Henry, Phys. Rev. E **62**, R1489 (2000).
- [6] F. Rouyer and N. Menon, Phys. Rev. Lett. **85**, 3676 (2000).
- [7] S. J. Moon, J. B. Swift, and H. L. Swinney, Phys. Rev. E **69**, 011301 (2004).
- [8] A. Baldassarri, U. M. B. Marconi, and A. Puglisi, Europhys. Lett. **58**, 14 (2002).
- [9] P. L. Krapivsky and E. Ben-Naim, J. Phys. A **35**, L147 (2002).
- [10] M. H. Ernst and R. Brito, Europhys. Lett. **58**, 182 (2002).
- [11] A. V. Bobylev and C. Cercignani, J. Stat. Phys. **106**, 547 (2002).
- [12] J. C. Maxwell, Phil. Trans. R. Soc. **157**, 49 (1867).
- [13] T. Pöschel and S. Luding (editors), *Granular Gases* (Springer, Berlin, 2000).
- [14] A. Rosas, J. Buceta, and K. Lindenberg, Phys. Rev. E **68**, 021303 (2003).
- [15] A. Rosas and K. Lindenberg, Phys. Rev. E **68**, 041304 (2003).
- [16] D. ben-Avraham, E. Ben-Naim, K. Lindenberg, and A. Rosas, Phys. Rev. E **68**, 050103(R) (2003).
- [17] V. F. Nesterenko, J. Appl. Mech. Tech. Phys. **5**, 733 (1983).
- [18] E. J. Hinch and S. Saint-Jean, Proc. R. Soc. London Ser. A **455**, 3201 (1999).
- [19] A. Rosas, D. ben-Avraham, and K. Lindenberg, in preparation.